# Predicting Multi-TeV Emission in Pulsars: Insights from *Fermi*-LAT 3rd Pulsar Catalog Phase-Resolved Spectral Analysis

**M. Regeard* & A. Djannati-Ataï & L. Dodeman**
**Université Paris Cité, CNRS, Astroparticule et Cosmologie, F-75013 Paris, France**

ICRC 2025
The Astroparticle Physics Conference
Geneva July 15-24, 2025

- Two pulsars detected at multi-TeV energies: Vela[1] and J1509–5850.
- Emission is interpreted as inverse Compton scattering of the electrons that produce the GeV emission seen with Fermi-LAT.
- Target photon fields span from near-infrared (NIR) through optical (O) to far-ultraviolet (FUV) wavelengths.
- Only a handful of pulsars detected in the optical band, owing to their faintness at these wavelengths.
- For Vela, extrapolating its X-ray spectrum[2] into the optical matches the measured flux remarkably well.
- Although J1509–5850 has no confirmed optical counterpart, extrapolation of its X-ray emission provides a sufficient photon field to account for the TeV signal seen by H.E.S.S.

**Figure 1:** SED and modeling of the GeV and TeV emission of the Vela pulsar. Figure 3 from 1

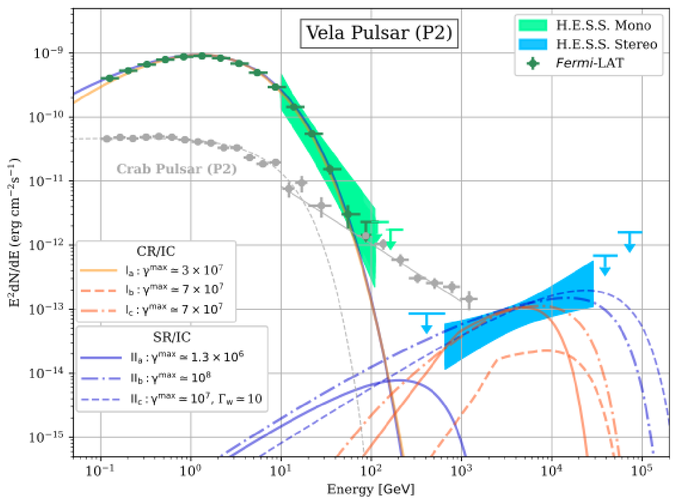


- Inverse Compton emission of Vela-like pulsars is mainly constrained by the underlying electron population which can be derived from Fermi-LAT data.
- Pulsed signals at very-high energies remain below the sensitivity of current IACTs, but next-generation observatories (CTAO, SWGO) will offer a promising reach.
- Our objective is is to produce a list of likely strong multi-TeV candidates for future detections

Analysis Workflow:
1. Pulsar selection
2. Fermi-LAT spectral analysis
3. Radiative modelling
4. Inverse Compton scattering

## ① Pulsar Selection

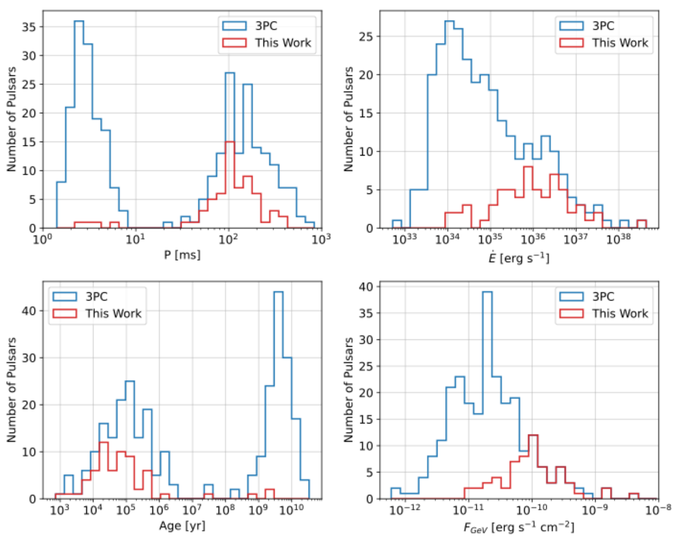


**Figure 2:** Selection of pulsars versus 3PC

- Selected pulsars from 3PC[3]: union of 50 brightest and 50 more luminous pulsars
- 15 pulsars removed: 63 pulsars selected
- 4 Millisecond Pulsars (MSPs) and 59 Young Pulsars (YPs)

## ② *Fermi*-LAT spectral analysis

2.1 Fermi-LAT On-Off analysis with Gammapy[4]:
- On-Off in pulsar rotational phase
- Energy range: 100 MeV to 1 TeV
- 10°×10° map centered on the pulsar position
- Events and Instrument Response Function (IRFs) pre-processed with FermiTools[5]

2.2 Defining On and Off phase range:
- Fit asymmetric Lorentzian and Gaussian to Fermi-LAT pulsed profiles
- On phase range taken as $2\sigma$ on each side of $\phi_0$
- Off region taken where there is no pulsed emission

$$\mathcal{G}(\phi) = A_0 \exp\left(\frac{-(\phi-\phi_0)^2}{2\sigma^2}\right)$$

$$\mathcal{L}(\phi) = \frac{A_0}{1+\left(\frac{\phi-\phi_0}{\sigma}\right)^2} \qquad \sigma = \sigma_L \text{ if } \phi < \phi_0 \text{ else } \sigma = \sigma_T$$

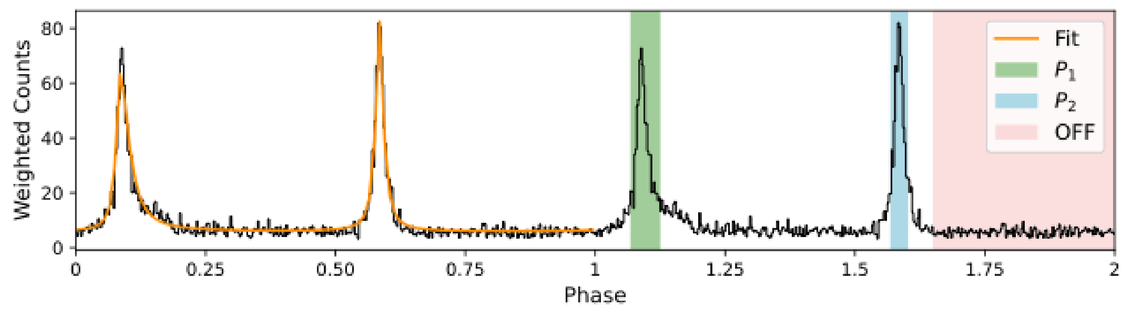


**Figure 3:** Phasogram with best-fit model, On and Off phase range

## ③ Radiative modeling

3.1 Pulsars without distance measurments:
- Derive $L_\gamma$ vs $\dot{E}$ relationship for pulsars with known distance in our sample

$$L_\gamma = 10^{19.891\pm0.105} \times \dot{E}^{0.412\pm0.003}$$

- Gives an estimate of unkown distances

3.2 Synchrotron and Curvature radiation
- Gammapy & Naima[7] interface
- UltraNest[8]: Fitting
- SR: $B = B_{LC}$ (fixed)
- CR: $R_c = R_{LC}$
- $e^-$ population: Exponential Cutoff Power-Law

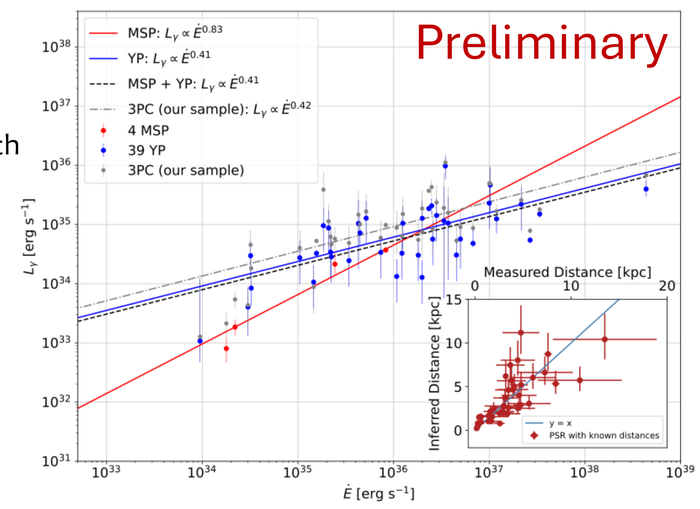


**Figure 4:** Distribution of $L_\gamma$ vs $\dot{E}$ and associated inferred distance vs measured distances

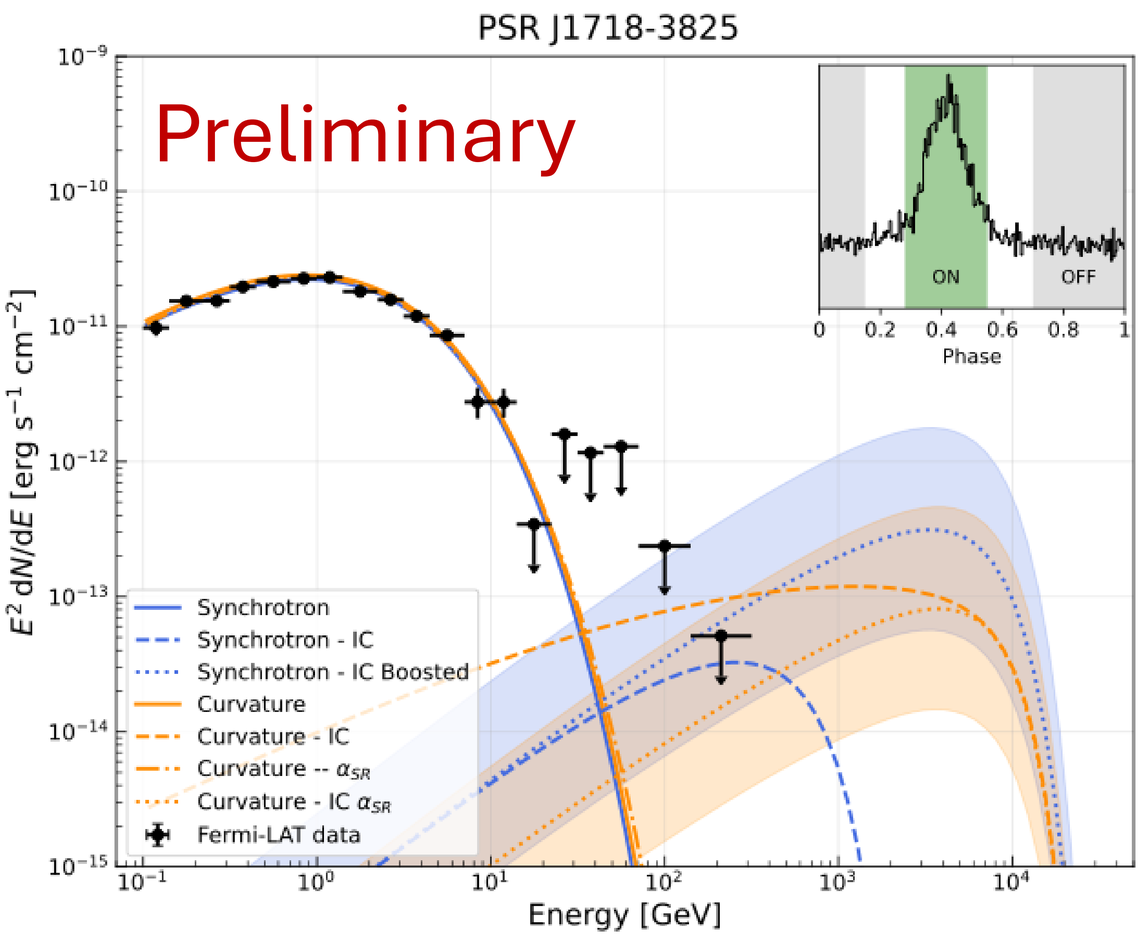


**Figure 6:** SED and modeling of Fermi-LAT data + inverse Compton prediction

## ④ Inverse Compton

4.1 X-ray extrapolation to the optical range
- Shibanov et al. 2003 → extrapolation of pulsed X-ray to the optical → high uncertainties due to $\Gamma_X$
- Provides decent targets to reproduce Vela and J1509-5850 TeV measurments.
- Search in the littérature for X-ray measurments of our pulsars: 35 pulsars

4.2 Producing inverse Compton:
- $e^-$ population fitted on *Fermi*-LAT data + target photon field from X-ray extrapolation
- SR: $E_{cut} < \gamma_{TeV}^{max}$ → Boost $E_{cut}$ based on Vela
- CR: Index too soft to reproduce TeV data: solved by fitting with synchrotron index: mocking SynchroCurvature[9] radiation
- Interaction volume:

$$V_{SR} \propto R_{LC}^2 \times R_{gyr} \qquad V_{CR} \propto R_{LC}^3$$

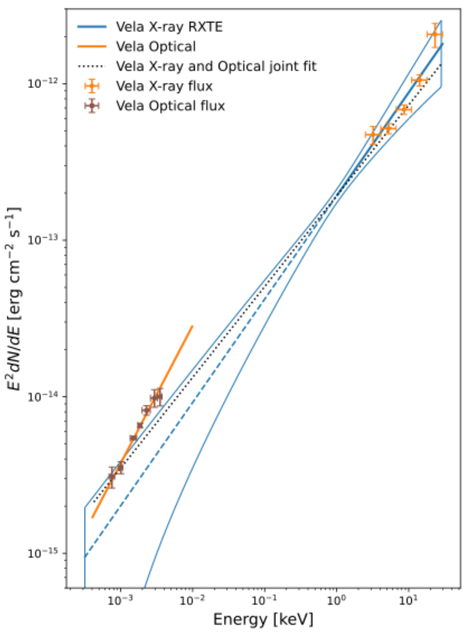


**Figure 5:** Extrapolation of Vela P2 pulsed X-ray to the optical range

| PSRJ | Peak | d kpc | $\Gamma_X$ | $L_X$ $10^{32}$ erg s$^{-1}$ | $L_O$ $10^{30}$ erg s$^{-1}$ | $E_c^{CR}$ TeV | Ref. |
|---|---|---|---|---|---|---|---|
| Potentially TeV-bright pulsars | | | | | | | |
| J1747-2958 | $P_1(P_2)$ | 4.75 | $1.55 \pm 0.04$ | [65.2 - 70.0]† | [169 - 289] | 13.1 | [3] |
| J1952+3252 | $P_2(P_1)$ | 3.00 | $1.63 \pm 0.05$ | [36.2 - 39.2]† | [161 - 318] | 12.9 | [4] |
| J1509-5850 | $P_1$ | 3.37 | $1.90 \pm 0.12$ | [0.93 - 1.04] | [19.6 - 108] | 19.9 | [6] |
| J1016-5857 | $P_2(P_1)$ | 3.16 | $1.72 \pm 0.11$ | [1.81 - 2.11] | [10.9 - 49.6] | 15.5 | [8] |
| J1709-4429 | $P_1$ | 2.60 | $1.67 \pm 0.20$ | [2.17 - 2.93] | [5.22 - 80.8] | 17.2 | [5] |
| J1809-2332 | $P_2(P_1)$ | 1.70 | $2.00 \pm 0.54$ | [0.61 - 0.89] | [1.48 - 3740] | 11.3 | [2] |
| J1718-3825 | $P_1$ | 3.48 | $1.47 \pm 0.21$ | [2.61 - 3.93] | [1.4 - 22.9] | 13.6 | [9] |
| J1028-5819 | $P_2(P_1)$ | 1.42 | $1.70 \pm 0.20$ | [0.38 - 0.50] | [1.12 - 17.6] | 6.5 | [1] |
| J1459-6053 | $P_1$ | 1.44 | $2.10 \pm 1.00$ | [0.23 - 0.38] | [0.04 - 99200] | 18 | [7] |
| Potentially TeV-faint pulsars | | | | | | | |
| J1826-1256 | $P_2(P_1)$ | 1.2 | $1.3 \pm 0.2$ | [33 - 52] | [0.06 - 0.8] | 19.7 | [13] |
| J1048-5832 | $P_2(P_1)$ | 2.9 | $1.46 \pm 0.34$ | [0.25 - 0.48] | [0.06 - 5.45] | 18.4 | [11] |
| J0007+7303 | $P_1$ | 1.4 | $1.3 \pm 0.18$ | [0.11 - 0.17] | [0.021 - 0.22] | 24.9 | [10] |
| J1420-6048 | $P_1$ | 5.6 | $0.7 \pm 0.4$ | [4.1 - 13] | [0.003 - 0.4] | 17.8 | [12] |
| J1838-0537 | $P_1$ | 2.11 | $0.8 \pm 0.2$ | [0.29 - 0.54] | [0.001 - 0.01] | 21.5 | [14] |

**Table 1:** Non exhaustive list of good candidate pulsars for multi-TeV emission. Associated index and luminosity in X-ray and extrapolated optical luminosity.
† High X-ray luminosity → Improbably high Optical luminosity

[1] Mignani, R. P. et al. (2012); [2] Van Etten et al. (2012); [3] Klingler et al. (2018); [4] Li et al. (2005); [5] Romani et al. (2005); [6] Klingler et al. (2016); [7] Pancrazi, B. et al. (2012); [8] Safi-Harb & Kumar (2008); [9] Van Etten et al. (2008); [8] Klingler et al. (2022); [9] Hinton et al. (2007); [10] Caraveo et al. (2010); [11] Danilenko et al. (2013); [12] ?; [13] Li et al. (2018); [14] Marelli et al. (2015)
1 Aharonian et al. (2023); 2 Shibanov et al. (2003); 3 Smith et al. (2023); 4 Donath et al. (2023); 5 Fermi Science Support Development Team (2019); 6 Abdollahi et al. (2022); 7 Zabalza (2015); 8 Buchner (2021); 9 Cheng & Zhang (1996);